PAIN

OPEN

Chronic neuropathic pain reduces opioid receptor availability with associated anhedonia in rat

Scott J. Thompson[a,b], Mark H. Pitcher[a,*], Laura S. Stone[b], Farid Tarum[a], Gang Niu[c], Xiaoyuan Chen[c], Dale O. Kiesewetter[c], Petra Schweinhardt[b], M. Catherine Bushnell[a]

Abstract

The opioid system plays a critical role in both the experience and management of pain. Although acute activation of the opioid system can lead to pain relief, the effects of chronic pain on the opioid system remain opaque. Cross-sectional positron emission tomography (PET) studies show reduced availability of brain opioid receptors in patients with chronic pain but are unable to (1) determine whether these changes are due to the chronic pain itself or due to preexisting or medication-induced differences in the endogenous opioid system, and (2) identify the neurobiological substrate of reduced opioid receptor availability. We investigated these possibilities using a well-controlled longitudinal study design in rat. Using [^{18}F]-FDPN-PET in either sham rats (n = 17) or spared nerve injury rats (n = 17), we confirmed reduced opioid receptor availability in the insula, caudate–putamen, and motor cortex of nerve injured rats 3 months after surgery, indicating that painful neuropathy altered the endogenous opioid system. Immunohistochemistry showed reduced expression of the mu-opioid receptor, MOR1, in the caudate–putamen and insula. Neither the opioid peptide enkephalin nor the neuronal marker NeuN differed between groups. In nerve-injured animals, sucrose preference, a measure of anhedonia/depression-like behavior, positively correlated with PET opioid receptor availability and MOR1-immunoreactivity in the caudate–putamen. These findings provide new evidence that the altered supraspinal opioid receptor availability observed in human patients with chronic pain may be a direct result of chronic pain. Moreover, reduced opioid receptor availability seems to reflect decreased receptor expression, which may contribute to pain-induced depression.

Keywords: Chronic pain, Opioid receptors, Anhedonia, Positron emission tomography, Rat

1. Introduction

Opioid analgesics are not equally efficacious for every patient with chronic pain.[8,12,38] Although mechanisms of interindividual differences in efficacy of opioid analgesics are largely unclear, mounting evidence from positron emission tomography (PET) studies in a variety of chronic pain conditions indicates that, compared with controls, patients have reduced opioid receptor availability in the brain.[7,18,21,25–27,30,32,50,55] However, cross-sectional studies in patients with variable genetics and exposure to analgesic medications are unable to reveal whether altered receptor availability is due to the chronic pain itself or due to either a preexisting or medication-induced difference in the endogenous opioid system. Furthermore, the neurobiological mechanism of reduced availability is equally unclear, where reduced receptor availability may be due to increased release of endogenous opioids occupying the receptors, reduced opioid receptor expression, or reduced numbers of opioid-expressing neurons. Indeed, although acute pain in healthy subjects can increase endogenous opioid levels in the brain,[6,50,60–62] it is also possible that either the pain or previous pain treatments reduces the number of opioid receptors, as observed in the spinal cord after nerve injury.[44,46,47,58] Alternatively, reduced availability may also result from a smaller number of opioid-expressing neurons. Reductions in gray matter occur in human patients with chronic pain[10,37] and in rats after nerve injury.[49] Diminished opioid receptor expression or neuronal loss both represent a fundamental remodeling in the brain that alters the capacity of those regions to respond to endogenous or exogenous opioids, and could underlie the lack of opioid efficacy in chronic pain.

Given the endogenous opioid system's central role in pain, reward, and addiction, changes to this system could also impact mental health. Both human patients with chronic pain and rodents sometimes exhibit anhedonia (an inability to derive pleasure from normally rewarding stimuli) as well as functional and anatomical changes in the reward system.[31,37,56] Thus, it is possible that reduced opioid receptor availability in chronic pain is related to the expression of anhedonia. These questions are best addressed using preclinical rodent models, where longitudinal studies controlling genetics, environment, and opioid exposure can be performed. We used a preclinical pain model along with

tools that allow for direct comparison with the clinical studies. We used the same clinical in vivo brain imaging tool (PET) and opioid tracer ([18F]-FDPN) in a rat model of intractable neuropathic pain (spared nerve injury [SNI]), so that tissue could be extracted and evaluated using immunohistochemistry to investigate the cellular and molecular basis of the observed changes.

2. Materials and methods

2.1. Overview

As summarized in **Figure 1**, all rats were processed as a single cohort with a minimum period of 48 hours between each procedure. In brief, rats underwent housing acclimation (3-4 weeks before surgery), baseline sucrose preference (2-3 weeks before surgery), baseline sensory testing (1 week before surgery), pain induction surgery or sham surgery (week 0), postsurgical sensory testing (week 1), 3-month sensory and behavior testing (weeks 11-12), PET brain imaging (weeks 12-13), and fixation (week 14). All procedures were approved by the National Institute of Health NINDS/NIDCD Animal Care and Use Committee. Standard procedures and precautions for working with radioactive materials were followed, and procedures were approved by the National Institute of Health Division of Radiation Safety.

2.2. Subjects

Forty-six male Sprague-Dawley rats (150-200 g; Charles River Laboratories, Frederick, MD) were pair housed (injured with injured and control with control) in temperature-controlled (21.7-23.3°C) ventilated racks on an inverted light/dark cycle (lights on from 21:00-09:00). Ad libitum access to both food (soy-free diet, Harlan Teklad 2020X) and water was provided. Thirty-four rats (SNI = 17 and sham = 17) completed all behavioral testing and FDPN-PET brain imaging. Brain tissue was processed for immunohistochemistry from 16 of these rats (SNI = 8 and sham = 8). Exclusion and inclusion criteria are listed within each respective section.

2.3. Neuropathic pain model

The SNI model of neuropathic pain is a well characterized model of peripheral neuropathic pain that results in persistent touch and temperature sensitivity on the injured paw.[16] For this study, rats were randomly assigned to either SNI (24 rats) or sham groups (22 rats, control group). For the procedure, rats were anesthetized with isoflurane (5.0% for induction and 2.0% for maintenance, 1 L/min). The surgery involves exposing the left sciatic nerve by blunt dissection of the biceps femoris muscle. The tibial and common peroneal nerves are ligated (2 on each nerve, 2-3 mm separation), and each is sectioned between the ligations. The sural nerve is left intact. Sham surgery (control) is identical with the exception that the sciatic nerve is visualized but not modified.

2.4. Sensory testing

Before behavioral testing, rats were habituated to the room for 1 hour in their home cages followed by a 30-minute habituation to the testing apparatus. Mechanical sensitivity was measured using a Dynamic Plantar Aesthesiometer (Ugo Basile, Varese, Italy) with a 50-g peak and 10-second ramp. Thirty minutes after, cold sensitivity was assessed with the acetone test.[13] Fifty microliters of acetone was applied to the plantar surface of the hind paw, and the duration of the response (shaking or licking of the paw) that occurred within 1 minute was measured with a stopwatch. One nerve-injured rat was excluded from sensory testing at the 3-month postsurgery time point because the plantar surface of the foot was not accessible with the testing apparatus.

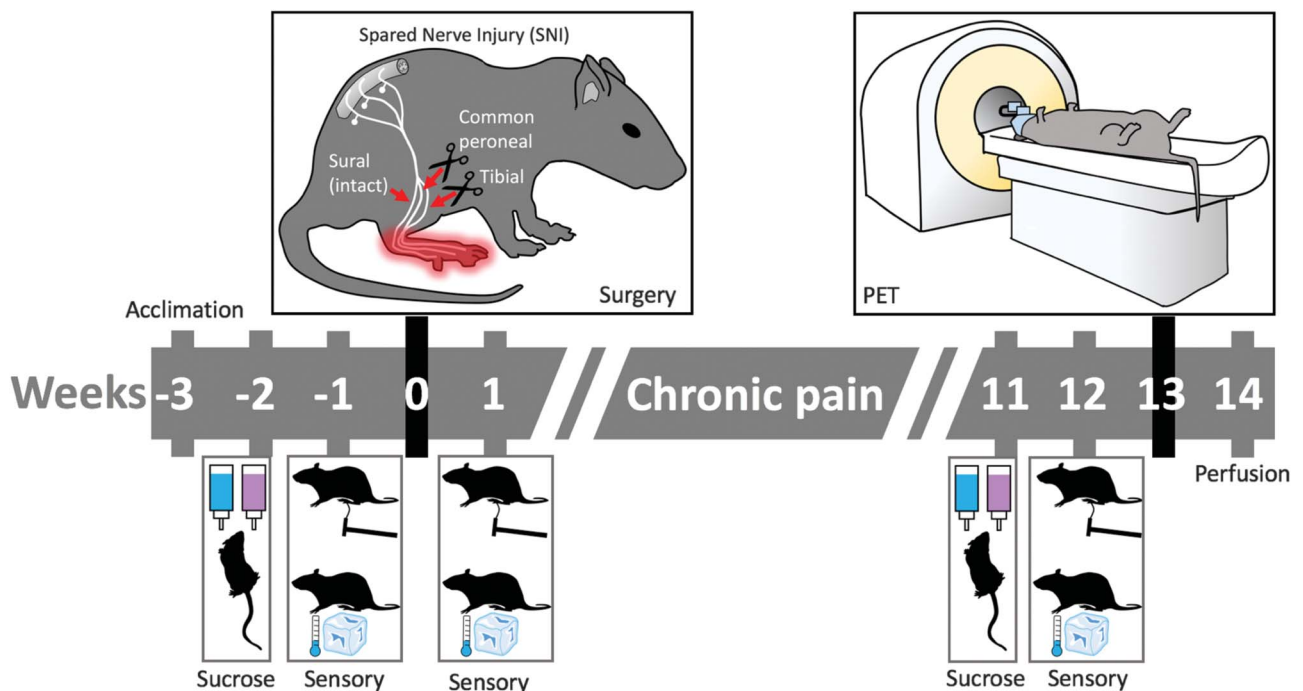**Figure 1.** Study design. Behavioral testing for mechanical and cold sensitivity was performed before surgery and again 1 week and 3 months after surgery. Rats were tested for sucrose preference as an index of anhedonia before surgery and again 3 months after surgery. [18F]FDPN-PET was performed at week 13 followed by tissue fixation for immunohistochemistry at week 14. PET, positron emission tomography.

2.5. Sucrose preference

Sucrose preference was used as a measure of anhedonia. Procedures similar to Amorim et al.[2] were followed. To familiarize the rats with the procedure, each rat was placed individually into a clean, empty cage for a period of 2 hours with 1 bottle of water and 1 bottle of 1% sucrose water for 5 consecutive days, alternating the side containing sucrose water daily to minimize learning effects. Three days later, food and water were removed from the home cage at 17:00. At 10:00 on the next day, each rat was placed into a clean cage with preweighed bottles of 1% sucrose water and water. After a period of 1 hour, the amount of liquid consumed was measured. Sucrose preference testing was repeated at 3 months after surgery. One sham rat was excluded from analysis as a result of a bottle leak during the baseline testing procedure. The sucrose preference score was calculated as the proportion of sucrose water consumed before surgery and 3 months after surgery: (sucrose water consumed/[sucrose water consumed + water consumed]) × 100.

2.6. Radiochemistry

We opted to use 6-O-(2-[^{18}F]fluoroethyl)-6-O-desmethyldi-prenorphine ([^{18}F]FDPN) based, in part, on the relatively long half-life and short positron range associated with the fluorine-18 (^{18}F) radioisotope. [^{18}F]FDPN is a radioactively labeled PET tracer that is an analog of diprenorphine with a half life of 110 minutes. Like diprenorphine, [^{18}F]FDPN is a nonselective opioid receptor antagonist that binds with equal affinity to mu, delta, and kappa. The synthesis followed the method of Wester et al[53] with some modifications. Specifically, [^{18}F] fluoroethyltosylate was made through an automated procedure. The automatic HPLC trace enrichment method for semipreparative HPLC of final product was not used; different HPLC columns and solid-phase extraction columns were used. Last, the final product was isolated from HPLC eluate using solid-phase extraction.

2.7. Positron emission tomography imaging

After 1 hour of acclimation to the PET facility, rats were placed in an anesthesia induction chamber with 5% sevoflurane. Rats were removed from the chamber, whereas anaesthesia was maintained with 3% sevoflurane administered through nose cone. Depth of anesthesia was confirmed by nonresponse to toe pinch. Rats were then given a tail-vein injection of the PET tracer [^{18}F] FDPN (0.6 mCi). Anesthetic was immediately removed, and the rats were placed in a 30 × 30 × 30 cm ventilated Plexiglas box. At minute 25 after injection, rats were removed from the Plexiglas box and anesthetized in an induction chamber with 5% sevoflurane followed by placement on the PET scanner bed (Inveon small-animal PET scanner; Siemens Healthcare, Erlangen, Germany) in a prone position and maintained under 3% sevoflurane anesthesia administered through nose cone. Body temperature was maintained with a heating pad, and sterile ophthalmic ointment was applied to the eyes to prevent desiccation under anaesthesia. Positron emission tomography scanning started at minute 30 after injection for a period of 30 minutes. Rats with incomplete behavioral data and their cage mates were excluded from PET imaging. In addition, one production of [18F]FDPN did not result in supraspinal binding, and there were 2 scan acquisition failures. In total, PET data for 17 SNI-operated rats and 17 sham-operated rats were collected and analyzed.

2.8. Positron emission tomography image processing and analysis

Image reconstruction was performed using Siemens microPET Manager Software. An OSEM3D (3 iterations) MAP (18 iterations) algorithm was used to create a single timeframe for the 30 minutes of data in a 128 × 128 × 159 matrix with a voxel size of 0.78 × 0.78 × 0.80 mm. The files were then converted from the proprietary manufacturer's image file format to the NIfTI file format using (X)MedCon (http://xmedcon.sourceforge.net/). To facilitate automated alignment, a block of 30 × 25 × 50 voxels centered on the thalamus and containing the whole brain was extracted from each scan.

Registration was performed using a combination of SPM8 (http://www.fil.ion.ucl.ac.uk/spm/software/spm8/) and minc tools (http://www.bic.mni.mcgill.ca/ServicesSoftware/MINC). The PET scans were aligned to a common space with SPM8 using the PET toolbox with a 1.6 mm smoothing kernel and linear registration algorithm. The group average of the PET scans was then converted to the minc file format to manually coregister a size-matched anatomical rat magnetic resonance imaging (MRI) to the PET space using the software "register."

Brain regions relevant to pain and reward were defined on the anatomical rat MRI in Paxinos space[40] to confirm that the tracer was binding as expected in the control rats. Regions of interest (ROIs) defined were the thalamus, anterior insula (Ant Ins), posterior insula (Post Ins), the prelimbic and infralimbic cortex (homologous to the human prefrontal cortex [PFC]), anterior Cg1 and Cg2 (homologous to the human anterior cingulate cortex [ACC]), nucleus accumbens (NAc), caudate–putamen (CPu), posterior Cg1 and Cg2 (homologous to human mid-cingulate cortex), amygdala, secondary somatosensory cortex (S2), visual cortex (V1/V2), periaqueductal gray (PAG), cerebellum, and the primary somatosensory cortex (S1). All regions have the right and left hemisphere defined separately with the exception of the cerebellum and a few brain regions located on the midline including PFC, PAG, ACC, and mid-cingulate cortex. Each PET scan was then normalized using the reference tissue ratio method with a cerebellum mask (eroded to minimize partial volume effects) used as the reference region. The ROI map was applied to each individual sham rat PET image to extract the mean, cerebellum normalized tracer binding within each region.

Group differences between SNI and sham-operated rats were evaluated using SPM8, investigating the contrast SNI < sham under the assumption that results would mimic the decrease in opioid receptor availability seen in the clinical PET chronic pain studies. This assumption was verified by checking the SNI > sham contrast. The resultant contrast maps were masked for z > 2.3 and cluster corrected using the SPM8 toolbox VBM8 to calculate the cluster size threshold for a resultant 1-tailed, cluster-corrected threshold of $P < 0.01$.

2.9. Perfusion fixation

From the 34 rats (SNI = 17 and sham = 17) that underwent FDPN-PET brain imaging, 16 (SNI = 8 and sham = 8) were selected by randomly choosing 1 rat from each cage followed by verification that there was no weight difference between the groups. Tissue fixation through intracardial perfusion was based on the procedures described by Arvidsson et al.[4] using a gravity fed system. In brief, animals were deeply anesthestized with isoflurane, the chest cavity was opened, the heart was exposed, a 15-gauge olive-tipped perfusion needle was inserted through the cut ventricle into the ascending aorta, and a relief incision was

made to the rat's right atrium. Perfusion consisted of 250 mL of vascular rinse (1 L = 50 mL of 0.2 M phosphate buffer solution [PBS] at pH = 7.4, 9 g NaCl, 0.25 g KCl, 0.5 g NaHCO3, and 950 mL distilled water) followed by 1000 mL of fixative (40 g paraformaldehyde diluted in 250 mL of distilled water, 400 mL of 0.4 M PBS, 140 mL of saturated picric acid, and 210 mL of distilled water at pH 6.9) and 500 mL of cryoprotection solution (10% sucrose in 0.2 M PBS). Rat brains were extracted and incubated in cryoprotection solution at 4°C for 5 days after fixation, embedded in optimal cutting temperature cutting medium (Tissue-Tek), and stored at −20°C.

2.10. Immunohistochemistry

From each rat, a total of 6 sections from each of the 2 coronal levels of interest were triple labeled to identify the mu-opioid receptor, enkephalin and neurons. Within those 2 coronal levels, 3 brain regions were selected for further analysis based on FDPN-PET results (see Results section: ipsilateral caudate-putamen, ipsilateral anterior insula, and contralateral posterior insula). Tissue was sectioned on a cryostat at a thickness of 14 μm with 126 μm spacing between each sample to span approximately 1 PET voxel width. The rabbit-derived MOR1 antisera were prepared against a synthetic peptide corresponding to $MOP_{384-398}$ (QLENLEAETAPLP) of the rat MOR1 gene and have been previously determined to be specific for MOR1 based on preadsorption studies, Western blot, and epitope-expressing cell lines.[4] The MOR1 antibody used here (RRID: AB_2314812; provided by Dr Lucy Vulchanova at the University of Minnesota) was harvested from the same rabbit used by Arvidsson et al.[4] and is well characterized in the opioid receptor research community. The mouse-derived anti-ENK antibody (MAB350; RRID: AB_2268028) and the guinea pig-derived anti-NeuN antibody (ABN90; RRID: AB_11205592) were acquired from EMD Millepore. Sections were washed in 0.01 M PBS then incubated in PBS containing blocking serum (1% normal donkey serum [Jackson ImmunoResearch Labs, West Grove, PA], 1% normal goat serum [Vector Lab, Burlingame, CA] +1% bovine serum albumin [Jackson ImmunoResearch Labs], and 0.3% Triton X-100) and the 3 antibodies (NeuN 1:1000; ENK 1:400; and MOR1 1:200) for 18 hours at 4°C. This was followed by incubation in PBS containing 3 separate secondary antibodies conjugated with Alexa Fluor 488, Alexa Fluor 594, and Alexa Fluor 350 (Invitrogen, Burlington, ON Canada). All steps were performed at room temperature except where indicated. Washes before and after each step were performed with 0.01 M PBS, 3 times, 3 minutes each. Finally, all sections were coverslipped by using Vectashield without DAPI (Vector Labs).

2.11. Microscopy

Images were collected on an Olympus BX51 fluorescent microscope (Olympus Corp, Tokyo, Japan). The filter cubes used for each respective fluorophore were Texas Red for Alexa Fluor 594, DAPI for Alexa Fluor 350, and FITC for Alexa Fluor 488. Images were acquired with a UPlanFL N, 20×/0.50, ∞/0.17/FN26.5 on an Olympus DP71 digital camera. Software used to record the images was the Olympus DP Controller 3.2.1.276 at an image size of 4080 × 3072, ISO sensitivity at 200, and saved as uncompressed TIFF. Acquisition time was kept constant across all rats for each section and label with exposure times established by testing sections of noninterest before data collection. Location of the ROIs was selected based on where the FDPN-PET results were observed (CPu, Bregma 1.68, vertical 3.8, and lateral −3.4; anterior insula, Bregma 1.68, vertical 3.8, and lateral −4.5; posterior insula, Bregma −0.72, vertical 3.2,

and lateral 6.3, stereotaxic coordinates, vertical orientation ventral to dorsal, and lateral orientation with left negative and right positive[40]).

2.12. Image analysis

Mu-opioid receptor expression was assessed using immunofluorescence intensity of the MOR1 antibody, similar to the methodology used by Ref. 59. Briefly, images were quantified using ImageJ v1.50, 64 bit. First, all images were converted to uncompressed grayscale TIFF images with immunofluorescence intensity levels represented by arbitrary units that fall within the range of the bit depth range of the digital camera. MOR1-immunoreactivity (-ir) and ENK-ir were quantified for mean intensity within the full image frame for all regions except the caudate–putamen, where the border between the caudate–putamen and anterior insula is within the image frame. Consequently, for the caudate–putamen, the mean intensity was assessed in the upper-right quadrant of the image (25% of the image, upper-right corner). NeuN cell bodies were counted by making the image binary, performing a watershed split and then performing a particle count with lower limit to the size of the particles set to 500 pixels to eliminate speckle noise from the output. As with MOR-ir and ENK-ir quantification, the NeuN-ir count was performed in the upper-right quadrant of the caudate–putamen images.

2.13. Experimental design and statistical analysis

2.13.1. Sensory and sucrose preference testing

Sample size was determined based on previous experience, with n = 45 (SNI = 23 and sham = 22) for sensory testing and n = 45 (SNI = 24 and sham = 21) for sucrose preference (exclusions listed in Methods section). The data were evaluated for outliers (3× interquartile range), normality (the Shapiro–Wilk test, $P <$ 0.05), and equal variance (Levene $P < 0.05$). A repeated-measures 2-way analysis of variance (ANOVA) was used to assess the data that occurred over multiple time points (2 time points for sucrose preference and 3 time points for all others), with time as a within-subject factor and surgical group as a between-subject factor. Post hoc tests using the Bonferroni correction were used to investigate between-subject differences. Given there is no nonparametric equivalent to a repeated-measures 2-way ANOVA, if the data did not meet the basic assumptions for parametric testing, the analysis was followed up with non-parametric Mann–Whitney U tests at each time point as an additional assessment of the data. Data were processed using SPSS (IBM SPSS, version 20.0.0), and results are reported as mean ± SE. Please refer to Section "Methods: Sensory testing; Sucrose preference" for complete details.

2.13.2. Positron emission tomography imaging and analysis

Sample size was determined based on previous experience, with n = 34 (SNI = 17 and sham = 17, exclusions listed in Methods section). Multiple comparisons for SNI vs sham contrast were controlled for by using cluster correction. Multiple comparisons for the sham ROI analysis (n = 17) were controlled for by using an ANOVA followed with post hoc Bonferroni correction. Data for the sham ROI analysis were processed using SPSS (IBM SPSS, version 20.0.0), and results are reported as mean ± SD. Please refer to Section "Methods: PET image processing and analysis" for complete details.
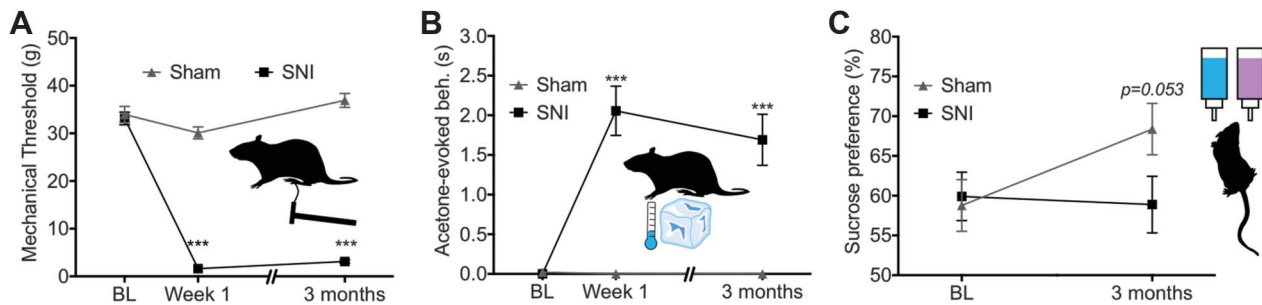
Figure 2. Neuropathic pain–induced deficits in hypersensitivity and anhedonia. (A) Repeated-measures 2-way ANOVA analysis of mechanical thresholds yielded a significant group × time effect ($F_{2,86} = 94.7$, $P < 0.001$). Although post hoc assessment showed no difference in mechanical threshold between the 2 groups before surgery, at both 1 week and 3 months after surgery, nerve-injured rats had a significantly lower withdrawal thresholds compared with controls. (B) A significant group × time effect ($F_{2,86} = 17.5$, $P < 0.001$) was also found for cold sensitivity. Post hoc analysis showed significant differences between groups at both postsurgery time points but not at baseline. (C) Repeated-measures 2-way ANOVA analysis of sucrose preference yielded a significant group × time effect ($F_{1,43} = 5.02$, $P = 0.030$). Data are presented as mean ± SEM. ***$P < 0.001$ compared with control group. ANOVA, analysis of variance; BL, baseline; SNI, spared nerve injury.

2.13.3. Microscopy image analysis

Sample size was determined based on previous experience with n = 16 (SNI = 8 and sham = 8, inclusion criteria listed in Methods section). A 2-way ANOVA was used to assess the effect of surgical group over the 3 brain regions for each of the quantified measures (anti-MOR1-ir, anti-ENK-ir, and NeuN cell count). Post hoc tests using the Bonferroni correction were used to investigate between-subject differences for each brain region. Data were processed using SPSS (IBM SPSS, version 20.0.0), and results are reported as mean ± SE. Please refer to Section "Methods: Microscopy; Image analysis" for complete details.

2.13.4. Brain and sucrose preference correlations

Correlations between opioid receptor–related measures within the caudate–putamen and sucrose preference were assessed with a 2-tailed bivariate Pearson correlation analysis. Data were processed using SPSS (IBM SPSS, version 20.0.0).

3. Results

3.1. Mechanical and cold hypersensitivity developed with nerve injury

Nerve-injured rats showed profound hypersensitivity to touch and cold 1 week after surgery that persisted at the 3-month postsurgery

time point (**Figs. 2A and B**). A significant group × time interaction was observed for mechanical threshold ($F_{2,86} = 94.7$, $P < 0.001$, **Fig. 2A**). Post hoc tests showed no significant presurgery mechanical threshold difference between the 2 groups with preoperation nerve-injured rats at 33.11 ± 1.32 g and preoperation control rats at 33.95 ± 1.70 g ($P = 0.698$). One week after operation, nerve-injured rats had a significantly lower withdrawal threshold at 1.63 ± 0.14 g compared with controls at 30.09 ± 1.26 g ($P < 0.001$). This difference persisted at the 3-month time point with nerve-injured rats' withdrawal threshold at 3.12 ± 0.36 g and controls at 36.92 ± 1.47 g ($P < 0.001$). Similarly, cold sensitivity showed a significant group × time interaction effect ($F_{2,86} = 17.5$, $P < 0.001$, **Fig. 2B**). There was no presurgery cold sensitivity difference (SNI = 0.00 ± 0.00 seconds, sham = 0.02 ± 0.02 seconds, $P = 0.154$). After surgery, a group difference was observed at 1 week (SNI = 2.06 ± 0.31 seconds, sham = 0.00 ± 0.00 seconds, $P < 0.001$) which persisted at the 3-month time point (SNI = 1.69 ± 0.32 seconds, sham = 0.00 ± 0.00 seconds, $P < 0.001$).

Because of an outlier and violation of normality and equal variance identified in the sensory data (outlier violation for 3-month cold sensitivity in nerve-injured rats; normality violations for 3-month mechanical sensitivity in nerve-injured rats, presurgery cold sensitivity in control rats, and 3-month cold sensitivity in nerve-injured rats; homogeneity of variance violations for cold and mechanical sensitivity for all time points except the 1-week mechanical sensitivity), the mixed ANOVAs were followed up by nonparametric Mann-Whitney
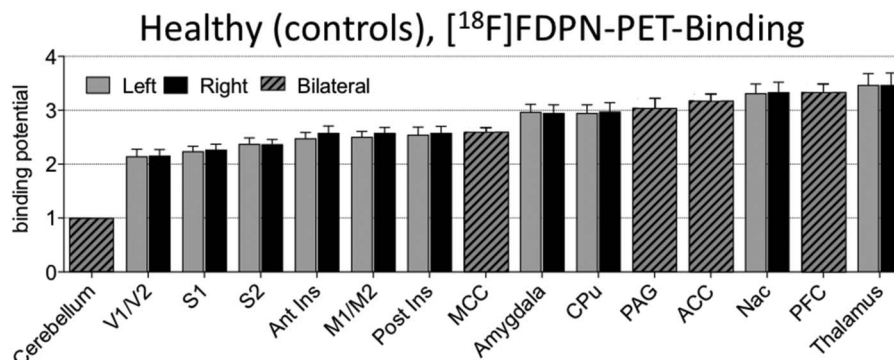

Figure 3. [^{18}F]-FDPN tracer binding in the control rat brain to validate the tracer. Values displayed are normalized with the cerebellum as reference region, mean ± SD. A 1-way ANOVA contrasting all brain regions was found to be significant $F_{22,368} = 284.251$, $P < 0.001$ with post hoc analysis contrasting each brain region to the cerebellum found each region to be significantly different from the cerebellum, which is devoid of opioid receptors ($P < 0.001$). ACC, anterior cingulate cortex; ANOVA, analysis of variance; MCC, mid-cingulate cortex; PAG, periaqueductal gray; PET, positron emission tomography; PFC, prefrontal cortex.
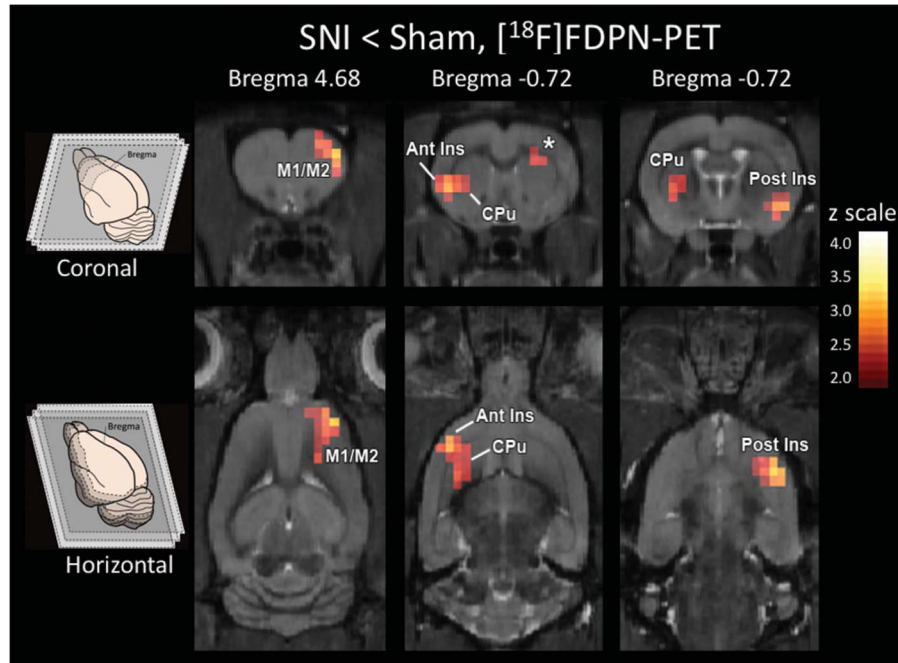
Figure 4. Reduced opioid receptor availability in the striatum. Less opioid receptor availability ($P < 0.01$, cluster corrected) was observed in nerve-injured rats than control rats in the ipsilateral anterior insula (Ant Ins), ipsilateral caudate–putamen (CPu), contralateral posterior insula (Post Ins), and contralateral M1/M2. There were no clusters or any single voxels that exceeded the significance threshold for the contrast of SNI > sham. SNI, spared nerve injury.

U tests at each time point. The outcomes did not change for any of the data assessed. Group differences for mechanical thresholds before surgery, 1 week after surgery, and 3 months after surgery had P values of 0.812, <0.001, and $P < 0.001$, respectively. P values for cold sensitivity before surgery, 1 week after surgery, and 3 months after surgery were 0.144, 0.001, and 0.001, respectively.

3.2. Sucrose preference decreased with nerve injury

Nerve-injured rats had lower sucrose preference than control animals 3 months after surgery, with no group differences in sucrose preference before surgery (**Fig. 2C**).

A repeated-measures 2-way ANOVA revealed a significant group × time interaction ($F_{1,43} = 5.02$, $P = 0.030$; presurgery SNI = 59.92 ± 3.04%, sham = 58.78 ± 2.35%; 3-month SNI = 58.88 ± 3.56%, sham = 68.38 ± 3.24%). Post hoc assessment looking at cross-sectional time points (which does not take into account the interindividual differences in sucrose preference) found that nerve-injured rats had a trend towards less sucrose preference than controls at the 3-month time point ($P = 0.057$) and no difference before surgery ($P = 0.800$). Because of potential divergence from normality (3-month percent sucrose consumed, $P = 0.011$), the nonparametric Mann–Whitney U test was used to compare nerve-injured with control rats before surgery, 3 months after surgery, and the difference scores (postsurgery minus presurgery sucrose preference for each individual rat to account for interindividual differences in sucrose preference). The nonparametric evaluation also suggests a significant group effect with time with presurgery $P = 0.856$, postsurgery $P = 0.053$, and the difference score $P = 0.014$.

3.3. Tracer distribution in controls

To validate the tracer methods, we examined binding levels in pain- and reward-related brain regions, many of which have high levels of opioid binding in humans.[5,23] In the control rats, we found specific binding of [18F]FDPN in all examined regions as shown in **Figure 3**. A 1-way ANOVA contrasting all examined brain regions showed an overall difference among sites ($F_{22,368} = 284.251$, $P < 0.001$). Post hoc analysis contrasting each brain region to the cerebellum (reference site) found each region to have significantly greater binding than the cerebellum, which is virtually devoid of opioid receptors[42] ($P < 0.001$). For the brain regions with right and left hemispheric data, an assessment of potential hemispheric differences using a 2-way ANOVA with brain region and hemisphere as factors showed no significant main effect for hemispheric side ($F_{1,288} = 1.799$, $P = 0.181$).

3.4. Opioid receptor availability decreased with nerve injury

Multiple brain regions showed less opioid receptor availability in the nerve-injured group (**Fig. 4**), whereas no brain region showed more opioid receptor availability (ie, increased tracer binding) in the nerve-injured group. The cluster threshold was calculated to be 14.341 voxels per cluster. Thresholding clusters to a minimum of 15 voxels, 3 clusters covering 4 brain regions were found to have significantly less FDPN tracer binding: the ipsilateral anterior insula and ipsilateral caudate–putamen (left side of the brain); the contralateral posterior insula; and the contralateral M1/M2. There were no clusters that exceeded the threshold for statistical inference for the contrast of SNI > sham, nor any single voxels with a voxel-based z-value greater than 2.3.

3.5. Immunohistochemistry

We extracted tissue from nerve-injured and control rats from regions showing pain-related reduced receptor availability that overlapped with the human literature (Ant CPu, Ant Insula, and Post Insula), and using immunohistochemistry, tissue was labeled for neuronal cell
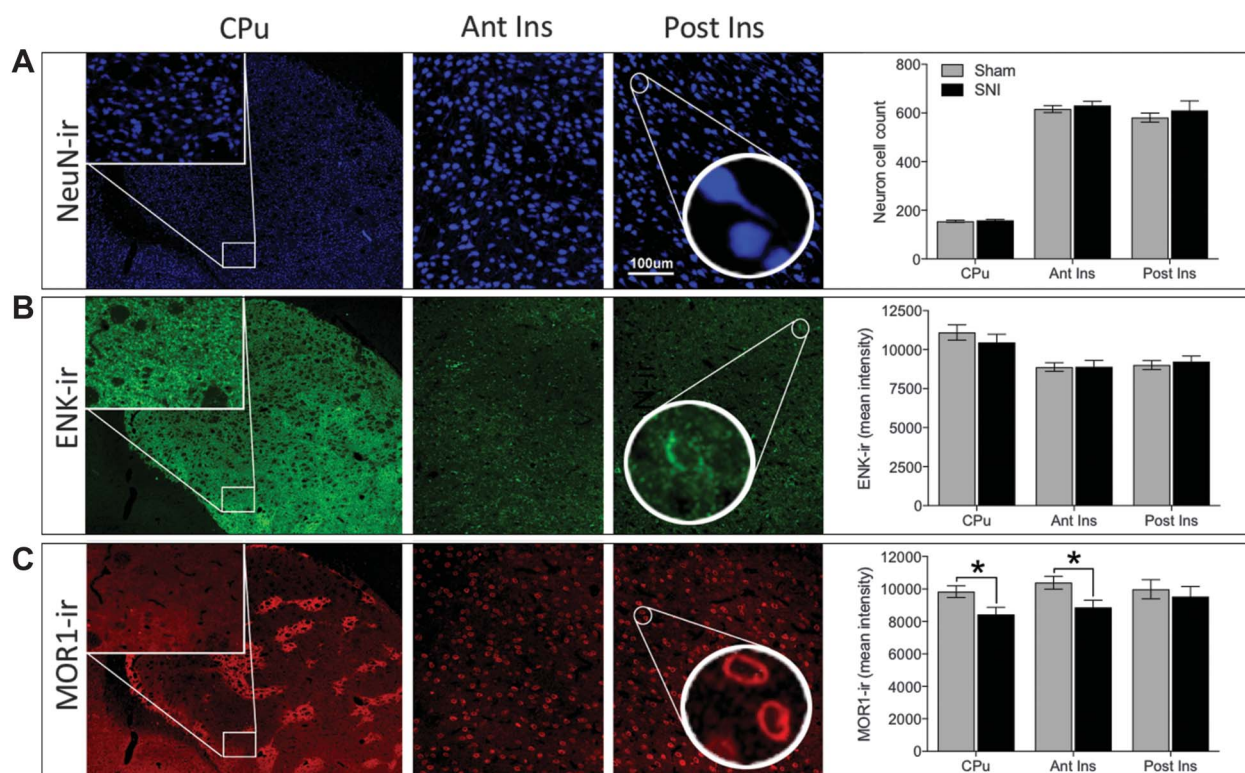
Figure 5. Reduced MOR1 expression in the striatum. (A) Representative images and quantification of NeuN-ir, neuron cell body count. Representative images taken from the caudate-putamen (CPu) at 4× magnification (insets at 20× represent region of CPu used for analysis), as well as the anterior insula (Ant Ins) and posterior insula (Post Ins) at 20× magnification. No significant difference in neuronal cell body count was observed between nerve-injured and control rats ($F_{1,42} = 0.936$, $P = 0.339$). (B) Representative images and quantification of ENK-ir (enkephalin immunoreactivity). No significant difference in ENK-ir was observed between nerve-injured and control rats ($F_{1,42} = 0.166$, $P = 0.685$). (C) Representative images and quantification of MOR1-ir (mu-opioid receptor immunoreactivity). A significant difference in MOR1-ir was observed between groups over 3 brain regions ($F_{1,42} = 8.092$, $P = 0.007$). Post hoc tests showed chronic pain to be associated with lower MOR1-ir intensity in 2 of the 3 brain regions: the CPu (SNI = 8437 ± 437; sham = 9832 ± 358; $P = 0.048$) and anterior insula (SNI = 8862 ± 452; sham = 10,390 ± 398; $P = 0.031$). The posterior insula (SNI = 9531 ± 620; sham = 9986 ± 587; $P = 0.510$) was not significantly different between groups. *$P < 0.05$. SNI, spared nerve injury.

bodies (NeuN), enkephalin (ENK), and mu-opioid receptors (MOR1) as shown in **Figure 5**.

3.5.1. Neuron count unchanged by nerve injury

The NeuN-ir cell count across the 3 brain regions was not significantly different between nerve-injured and control rats (**Fig. 5A**, $F_{1,42} = 0.936$, $P = 0.339$). Despite the negative result of the ANOVA, we performed post hoc tests for the individual brain region to demonstrate the lack of any trend (CPu [SNI = 159 ± 4; sham = 155 ± 5; $P = 0.882$], anterior insula [SNI = 630 ± 17; sham = 616 ± 15; $P = 0.627$], and posterior insula [SNI = 610 ± 40; sham = 580 ± 18; $P = 0.306$]).

3.5.2. Enkephalin-immunoreactivity unchanged by nerve injury

No difference in ENK-ir was observed over 3 brain regions (**Fig. 5B**, $F_{1,42} = 0.166$, $P = 0.685$), and none of the regions demonstrated any trend for a group difference (CPu [SNI = 10,464 ± 525; sham = 11,097 ± 487; $P = 0.271$], anterior insula [SNI = 8896 ± 412; sham = 8884 ± 273; $P = 0.983$], and posterior insula [SNI = 9232 ± 357; sham = 9014 ± 286; $P = 0.702$]).

3.5.3. Mu-opioid receptor immunoreactivity decreased with nerve injury

MOR1-ir across 3 brain regions differed between nerve-injured and control animals (**Fig. 5C**, $F_{1,42} = 8.092$, $P = 0.007$). Post hoc

tests showed lower mu-opioid receptor label intensity in the CPu as well as anterior insula in nerve-injured animals (CPu [SNI = 8437 ± 437; sham = 9832 ± 358; $P = 0.048$] and anterior insula [SNI = 8862 ± 452; sham = 10,390 ± 398; $P = 0.031$]). The posterior insula was not found to be significantly different between groups (SNI = 9531 ± 620; sham = 9986 ± 587; $P = 0.510$).

3.6. Sucrose preference was correlated with opioid receptor availability and MOR-ir

The proportion of sucrose water consumed at the 3-month time point for all rats was positively correlated with opioid receptor availability in the caudate–putamen cluster ($R = 0.353$, $P = 0.041$). As a secondary check, the relationship between the anatomically defined caudate–putamen and sucrose preference was investigated and was found to be significant ($R = 0.360$, $P = 0.037$). When the surgical groups were analyzed separately, the nerve-injured animals continued to show a positive correlation between sucrose preference and MOR-ir ($R = 0.500$, $P = 0.041$; **Fig. 6A**). By contrast, the sham group did not show this correlation ($R = 0.169$, $P = 0.515$).

The proportion of sucrose water consumed for all rats was also positively correlated with MOR1-ir in the caudate-putamen ($R = 0.628$, $P = 0.009$). When the surgical groups were analyzed separately, the SNI group continued to have a positive correlation for the CPu as shown in **Figure 6B** ($R = 0.799$, $P = 0.017$); however, the sham group did not ($R = -0.182$, $P = 0.667$).
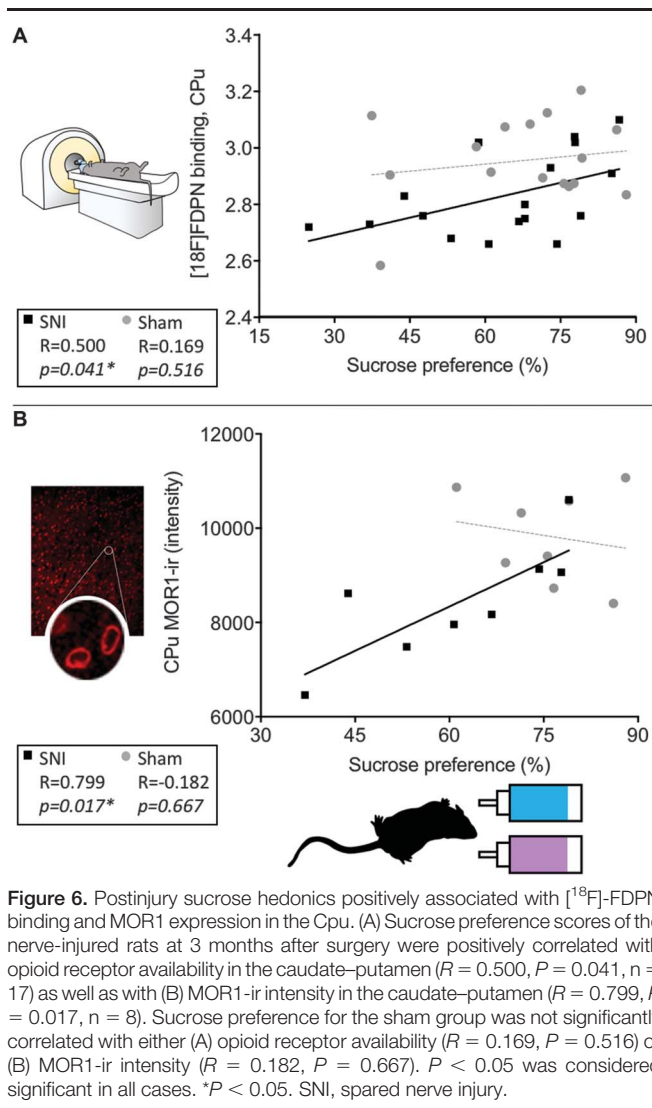
Figure 6. Postinjury sucrose hedonics positively associated with [^{18}F]-FDPN binding and MOR1 expression in the Cpu. (A) Sucrose preference scores of the nerve-injured rats at 3 months after surgery were positively correlated with opioid receptor availability in the caudate–putamen ($R = 0.500$, $P = 0.041$, n = 17) as well as with (B) MOR1-ir intensity in the caudate–putamen ($R = 0.799$, $P = 0.017$, n = 8). Sucrose preference for the sham group was not significantly correlated with either (A) opioid receptor availability ($R = 0.169$, $P = 0.516$) or (B) MOR1-ir intensity ($R = 0.182$, $P = 0.667$). $P < 0.05$ was considered significant in all cases. *$P < 0.05$. SNI, spared nerve injury.

4. Discussion

Our results show that after 3 months of hypersensitivity, nerve-injured rats have decreased opioid receptor availability in the insula, caudate–putamen, and motor cortex compared with matched sham controls. Ex vivo immunohistochemistry revealed decreased MOR1-ir in the anterior insula and caudate–putamen. Finally, sucrose preference, a rodent assay for anhedonia, positively correlated with opioid receptor availability and MOR1-ir in the caudate–putamen of the injured rats.

4.1. Chronic pain drives reductions in opioid receptor availability in the striatum and insula

Human cross-sectional studies showing reduced opioid binding in patients with chronic pain cannot determine whether reduced binding is caused by the pain condition, pain treatments, or represents an intrinsic brain difference in people who might be prone to develop chronic pain. To resolve this issue, we randomly assigned rats in this study to either the control or the injury condition, and ensured identical environmental conditions between groups. Opioid receptor availability was reduced in the nerve-injured group compared with controls, clearly indicating that reduced receptor availability is a result of the nerve injury. In this light, reduced opioid receptor availability in patients may also

be at least partially a direct consequence of chronic pain, especially in the subset exhibiting comorbid anhedonia.

As mentioned, a number of clinical studies have investigated opioid receptor availability in patients with chronic pain.[7,18,21,25–27,32,55] Of these, the most relevant comparison with our study is an investigation of patients with peripheral neuropathic pain using the PET tracer [^{11}C]diprenorphine.[32] As in this study, lower opioid receptor availability was found in the striatum and insula. Lower binding was also seen in the thalamus, ACC, posterior temporal and orbitofrontal cortices, and posterior midbrain. Although the differences observed by Maarrawi et al. were more widespread, the striatum and the insula are among the regions with the most consistently reduced opioid receptor availability across chronic pain conditions.[7,18,21,25–27,32,55] Thus, the reduced binding observed in this study strongly supports findings from human patients with chronic pain, whereas the changes in M1/M2 are unique to this study. Motor cortex findings may be due to partial volume effects of the small region size in immediate proximity to the ACC, a region rich in opioid receptors, or may be specific to the SNI model, which involves a partial sectioning of the sciatic nerve.

The distribution of the tracer binding observed here in controls is in line with previous findings in rodents and humans, suggesting a reasonably high interspecies homology. Specifically, of the brain regions investigated, the highest levels of binding were found in regions known to be densely populated with opioid receptors including the thalamus, PFC, NAc, ACC, PAG, CPu, and amygdala, whereas the lowest levels were seen in the sensory cortex, visual cortex, and cerebellum. Our findings in rat, together with others,[33,42] suggest that these opioid receptor–dense regions in the rat brain correspond to homologous regions in the human brain including the thalamus, ACC, caudate–putamen, and amygdala.[5]

4.2. Decreased opioid receptor availability reflects reduced receptor expression

As described in Section 1, there are several potential mechanisms underlying reduced opioid binding. These possibilities can only be discerned by examining the brain tissue where differences were observed with PET. We found reduced mu-opioid receptor immunoreactivity, likely indicating reduced receptor density, without significant reductions in enkephalin content or in the number of neurons.

Anatomical MRI studies in humans[11] and rodents[49] have demonstrated that a consistent pattern of gray matter decreases with chronic pain. However, our current findings, based on immunohistochemical labeling of neuronal markers, do not support the notion of pain-related neurodegeneration in the ROIs. Indeed, although one possible explanation for the gray matter decreases is neuronal loss, a recent study suggests that the more likely explanation involves changes in brain water content and neuronal integrity, rather than clear neuronal loss,[45] suggesting that the apparent discrepancy may be related to technical differences.

Although there is no direct evidence of increased levels of endogenous enkephalin in human patients with chronic pain, some have argued that higher levels of endogenously released enkephalin underlie decreased receptor availability in chronic pain states.[25,26] Studies of supraspinal enkephalin concentrations in rodent models of chronic pain focus mainly on brainstem nuclei including the PAG and the rostroventral medulla, where enkephalin levels seem to be transiently increased for no more than 3 weeks after CFA-induced persistent inflammation.[24,35,39,54] In higher brain regions such as the

hypothalamus, transient increases in enkephalin also return to basal levels by approximately 3 weeks.[39] In this study, no differences in enkephalin were observed in either the caudate–putamen or the insula 3 months after nerve injury, suggesting that although relatively short-term changes in endogenous enkephalin levels may occur in rodent models of chronic pain, these increases likely subside despite ongoing hypersensitivity. In the context of our findings, pain-related reduced receptor availability is unlikely to be related to increased enkephalin levels.

Downregulation of mu-opioid receptors in the rodent spinal cord and dorsal root ganglion can occur within days or a few weeks after nerve injury.[44,46,47,58] Our study extends these findings to the brain, suggesting that downregulation of mu-opioid receptors occurs throughout the central nervous system after nerve injury. Although we observed significant changes in the mu-opioid receptor system using immunohistochemistry in 2 of the 3 regions, it is important to note that [18F]FDPN binds to mu-, delta-, and kappa-opioid receptors with equal affinity. Accordingly, it is possible that delta- and kappa-opioids might also contribute to the lower opioid receptor availability observed with PET. Given that no statistically significant changes in MOR1-ir were found within the posterior insula, investigation of the delta- and kappa-opioid receptor within this region would be a logical extension of this work. However, of the aforementioned human opioid-PET studies investigating chronic pain, no systematic difference exists between those using [18F]FDPN and those using a carfentanil-based tracer (which binds specifically to the mu-opioid receptor), suggesting that the mu-opioid receptor system is a significant driver of this effect. As such, it is likely that the changes to the mu-opioid receptor give rise to the observed [18F]FDPN-PET changes. Taken together, our results strongly support altered expression levels of the mu-opioid receptor as the basis for the observed changes in opioid receptor availability using [18F]FDPN-PET.

4.3. Anhedonia and chronic pain

Sucrose preference, an assay for anhedonia, was lower in nerve-injured rats compared with controls after 3 months of nerve injury, in line with previous reports in rodent chronic pain models.[2,9,52] Preference for sweet-tasting water progressively increases with age in adult rats,[3,14,41] an effect that can be prevented by nerve injury.[3] Our findings match this pattern perfectly, where sucrose preference increased in controls but not in nerve-injured rats.

At 3 months after surgery, sucrose preference positively correlated with opioid receptor availability and MOR1-ir in the caudate–putamen of the injured rats. Specifically, although some nerve-injured rats exhibited sucrose preference levels and MOR1 expression that were comparable with sham rats, others showed lower levels of receptor expression along with marked anhedonia. As such, our results seem to correspond with the clinical findings that only a portion of the chronic pain population is depressed.[15,36,51] Moreover, although the caudate–putamen is known to play a role in anhedonia/depression[19,22,43] and trait anhedonia correlates with anterior caudate volume in humans,[22] the striatal opioid system, including the caudate–putamen, can modulate sucrose hedonics and feeding behavior in rats.[28,57] Therefore, as observed here in rats, the degree of anhedonia/depression observed in human patients with chronic pain may also be related to the level of mu-opioid receptor expression in the striatum. Interestingly, although we did observe pain-induced changes to anhedonia that correlated with opioid markers, we did not observe any correlation between hypersensitivity outcomes and opioid markers (post hoc exploration, data not reported). An intriguing extension to this work would be to attempt to

understand the interindividual differences in anhedonia, given that no linear relationship is observed between nociceptive assays and opioid markers.

Stress, especially chronic stress, is considered to be among the best indicators for the development of affective disorders in humans (reviewed in Refs. 20, 29), and comorbid depression has long been posited to be a direct consequence of chronic pain.[17,34] Here, we provide new evidence that chronic neuropathic pain changes the brain opioid system in rats. Moreover, the degree to which the opioid system is impacted corresponds to the level of anhedonia, a core symptom of major depression in humans.[1] Given the central role that opioid receptors play in pain, reward, and addiction, as well as the time-dependent impact of stress on anhedonia,[48] it is not surprising that persistent pain could, over time, affect one's ability to experience pleasure. With the current medical and political controversy regarding the use of opioids in patients with chronic pain, improved understanding of the relationship between chronic pain and the endogenous opioid system is crucial to better address issues related to opiate efficacy, addiction, and reward.

Conflict of interest statement

The authors have no conflict of interest to declare.

Supplemental video content

Video content associated with this article can be found online at http://links.lww.com/PAIN/A588.

References

[1] American Psychiatric Association. Diagnostic and statistical manual of mental disorders. 5th ed. Washington, DC: American Psychiatric Association, 2013.

[2] Amorim D, David-Pereira A, Pertovaara A, Almeida A, Pinto-Ribeiro F. Amitriptyline reverses hyperalgesia and improves associated mood-like disorders in a model of experimental monoarthritis. Behav Brain Res 2014;265:12–21.

[3] Andersen ML, Hoshino K, Tufik S. Increased susceptibility to development of anhedonia in rats with chronic peripheral nerve injury: involvement of sleep deprivation? Prog Neuropsychopharmacol Biol Psychiatry 2009;33:960–6.

[4] Arvidsson U, Riedl M, Chakrabarti S, Lee JH, Nakano AH, Dado RJ, Loh HH, Law PY, Wessendorf MW, Elde R. Distribution and targeting of a mu-opioid receptor (MOR1) in brain and spinal cord. J Neurosci 1995;15:3328–41.

[5] Baumgartner U, Buchholz HG, Bellosevich A, Magerl W, Siessmeier T, Rolke R, Hohnemann S, Piel M, Rosch F, Wester HJ, Henriksen G, Stoeter P, Bartenstein P, Treede RD, Schreckenberger M. High opiate

receptor binding potential in the human lateral pain system. Neuroimage 2006;30:692–9.

[6] Bencherif B, Fuchs PN, Sheth R, Dannals RF, Campbell JN, Frost JJ. Pain activation of human supraspinal opioid pathways as demonstrated by [11C]-carfentanil and positron emission tomography (PET). PAIN 2002; 99:589–98.

[7] Brown CA, Matthews J, Fairclough M, McMahon A, Barnett E, Al-Kaysi A, El-Deredy W, Jones AK. Striatal opioid receptor availability is related to acute and chronic pain perception in arthritis: does opioid adaptation increase resilience to chronic pain? PAIN 2015;156:2267–75.

[8] Bruehl S, Apkarian AV, Ballantyne JC, Berger A, Borsook D, Chen WG, Farrar JT, Haythornthwaite JA, Horn SD, Iadarola MJ, Inturrisi CE, Lao L, Mackey S, Mao J, Sawczuk A, Uhl GR, Witter J, Woolf CJ, Zubieta JK, Lin Y. Personalized medicine and opioid analgesic prescribing for chronic pain: opportunities and challenges. J Pain 2013;14:103–13.

[9] Bura AS, Guegan T, Zamanillo D, Vela JM, Maldonado R. Operant self-administration of a sigma ligand improves nociceptive and emotional manifestations of neuropathic pain. Eur J Pain 2013;17:832–43.

[10] Bushnell MC, Ceko M, Low LA. Cognitive and emotional control of pain and its disruption in chronic pain. Nat Rev Neurosci 2013;14:502–11.

[11] Cauda F, Palermo S, Costa T, Torta R, Duca S, Vercelli U, Geminiani G, Torta DM. Gray matter alterations in chronic pain: a network-oriented meta-analytic approach. Neuroimage Clin 2014;4:676–86.

[12] Chen L, Vo T, Seefeld L, Malarick C, Houghton M, Ahmed S, Zhang Y, Cohen A, Retamozo C, St Hilaire K, Zhang V, Mao J. Lack of correlation between opioid dose adjustment and pain score change in a group of chronic pain patients. J Pain 2013;14:384–92.

[13] Choi Y, Yoon YW, Na HS, Kim SH, Chung JM. Behavioral signs of ongoing pain and cold allodynia in a rat model of neuropathic pain. PAIN 1994;59:369–76.

[14] Colavita FB. Saccharine preference in rats as a function of age and early experience. Psychon Sci 1968;12:311.

[15] Currie SR, Wang J. Chronic back pain and major depression in the general Canadian population. PAIN 2004;107:54–60.

[16] Decosterd I, Woolf CJ. Spared nerve injury: an animal model of persistent peripheral neuropathic pain. PAIN 2000;87:149–58.

[17] Dohrenwend BP, Raphael KG, Marbach JJ, Gallagher RM. Why is depression comorbid with chronic myofascial face pain? A family study test of alternative hypotheses. PAIN 1999;83:183–92.

[18] Dossantos MF, Martikainen IK, Nascimento TD, Love TM, Deboer MD, Maslowski EC, Monteiro AA, Vincent MB, Zubieta JK, Dasilva AF. Reduced basal ganglia mu-opioid receptor availability in trigeminal neuropathic pain: a pilot study. Mol Pain 2012;8:74.

[19] Dunn RT, Kimbrell TA, Ketter TA, Frye MA, Willis MW, Luckenbaugh DA, Post RM. Principal components of the beck depression inventory and regional cerebral metabolism in unipolar and bipolar depression. Biol Psychiatry 2002;51:387–99.

[20] Hammen C. Stress and depression. Annu Rev Clin Psychol 2005;1: 293–319.

[21] Harris RE, Clauw DJ, Scott DJ, McLean SA, Gracely RH, Zubieta JK. Decreased central mu-opioid receptor availability in fibromyalgia. J Neurosci 2007;27:10000–6.

[22] Harvey PO, Pruessner J, Czechowska Y, Lepage M. Individual differences in trait anhedonia: a structural and functional magnetic resonance imaging study in non-clinical subjects. Mol Psychiatry 2007; 12:703, 767–75.

[23] Hirvonen J, Aalto S, Hagelberg N, Maksimow A, Ingman K, Oikonen V, Virkkala J, Nagren K, Scheinin H. Measurement of central mu-opioid receptor binding in vivo with PET and [11C]carfentanil: a test-retest study in healthy subjects. Eur J Nucl Med Mol Imaging 2009;36:275–86.

[24] Hurley RW, Hammond DL. Contribution of endogenous enkephalins to the enhanced analgesic effects of supraspinal mu opioid receptor agonists after inflammatory injury. J Neurosci 2001;21:2536–45.

[25] Jones AK, Cunningham VJ, Ha-Kawa S, Fujiwara T, Luthra SK, Silva S, Derbyshire S, Jones T. Changes in central opioid receptor binding in relation to inflammation and pain in patients with rheumatoid arthritis. Br J Rheumatol 1994;33:909–16.

[26] Jones AK, Kitchen ND, Watabe H, Cunningham VJ, Jones T, Luthra SK, Thomas DG. Measurement of changes in opioid receptor binding in vivo during trigeminal neuralgic pain using [11C] diprenorphine and positron emission tomography. J Cereb Blood flow Metab 1999;19:803–8.

[27] Jones AK, Watabe H, Cunningham VJ, Jones T. Cerebral decreases in opioid receptor binding in patients with central neuropathic pain measured by [11C]diprenorphine binding and PET. Eur J Pain 2004;8: 479–85.

[28] Kelley AE, Bakshi VP, Haber SN, Steininger TL, Will MJ, Zhang M. Opioid modulation of taste hedonics within the ventral striatum. Physiol Behav 2002;76:365–77.

[29] Kessler RC. The effects of stressful life events on depression. Annu Rev Psychol 1997;48:191–214.

[30] Klega A, Eberle T, Buchholz HG, Maus S, Maihofner C, Schreckenberger M, Birklein F. Central opioidergic neurotransmission in complex regional pain syndrome. Neurology 2010;75:129–36.

[31] Liu YT, Shao YW, Yen CT, Shaw FZ. Acid-induced hyperalgesia and anxio-depressive comorbidity in rats. Physiol Behav 2014;131:105–10.

[32] Maarrawi J, Peyron R, Mertens P, Costes N, Magnin M, Sindou M, Laurent B, Garcia-Larrea L. Differential brain opioid receptor availability in central and peripheral neuropathic pain. PAIN 2007;127:183–94.

[33] Melichar JK, Hume SP, Williams TM, Daglish MR, Taylor LG, Ahmad R, Malizia AL, Brooks DJ, Myles JS, Lingford-Hughes A, Nutt DJ. Using [11C]diprenorphine to image opioid receptor occupancy by methadone in opioid addiction: clinical and preclinical studies. J Pharmacol Exp Ther 2005;312:309–15.

[34] Merikangas KR, Risch NJ, Merikangas JR, Weissman MM, Kidd KK. Migraine and depression: association and familial transmission. J Psychiatr Res 1988;22:119–29.

[35] Millan MJ, Morris BJ, Colpaert FC, Herz A. A model of chronic pain in the rat: high-resolution neuroanatomical approach identifies alterations in multiple opioid systems in the periaqueductal grey. Brain Res 1987;416:349–53.

[36] Miller LR, Cano A. Comorbid chronic pain and depression: who is at risk? J Pain 2009;10:619–27.

[37] Navratilova E, Porreca F. Reward and motivation in pain and pain relief. Nat Neurosci 2014;17:1304–12.

[38] Noble M, Treadwell JR, Tregear SJ, Coates VH, Wiffen PJ, Akafomo C, Schoelles KM. Long-term opioid management for chronic noncancer pain. Cochrane Database Syst Rev 2010:CD006605.

[39] Panerai AE, Sacerdote P, Bianchi M, Brini A, Mantegazza P. Brain and spinal cord neuropeptides in adjuvant induced arthritis in rats. Life Sci 1987;41:1297–303.

[40] Paxinos G, Watson C. The rat brain in stereotaxic coordinates. Amsterdam, Boston (MA): Academic Press/Elsevier, 2007.

[41] Perez C, Sclafani A. Developmental changes in sugar and starch taste preferences in young rats. Physiol Behav 1990;48:7–12.

[42] Pert CB, Snyder SH. Opiate receptor: demonstration in nervous tissue. Science 1973;179:1011–14.

[43] Pizzagalli DA, Holmes AJ, Dillon DG, Goetz EL, Birk JL, Bogdan R, Dougherty DD, Iosifescu DV, Rauch SL, Fava M. Reduced caudate and nucleus accumbens response to rewards in unmedicated individuals with major depressive disorder. Am J Psychiatry 2009;166:702–10.

[44] Pol O, Murtra P, Caracuel L, Valverde O, Puig MM, Maldonado R. Expression of opioid receptors and c-fos in CB1 knockout mice exposed to neuropathic pain. Neuropharmacology 2006;50:123–32.

[45] Pomares FB, Funck T, Feier NA, Roy S, Daigle-Martel A, Ceko M, Narayanan S, Araujo D, Thiel A, Stikov N, Fitzcharles MA, Schweinhardt P. Histological underpinnings of grey matter changes in fibromyalgia investigated using multimodal brain imaging. J Neurosci 2017;37: 1090–101.

[46] Porreca F, Tang QB, Bian D, Riedl M, Elde R, Lai J. Spinal opioid mu receptor expression in lumbar spinal cord of rats following nerve injury. Brain Res 1998;795:197–203.

[47] Rashid MH, Inoue M, Toda K, Ueda H. Loss of peripheral morphine analgesia contributes to the reduced effectiveness of systemic morphine in neuropathic pain. J Pharmacol Exp Ther 2004;309:380–7.

[48] Rygula R, Abumaria N, Flugge G, Fuchs E, Ruther E, Havemann-Reinecke U. Anhedonia and motivational deficits in rats: impact of chronic social stress. Behav Brain Res 2005;162:127–34.

[49] Seminowicz DA, Laferriere AL, Millecamps M, Yu JS, Coderre TJ, Bushnell MC. MRI structural brain changes associated with sensory and emotional function in a rat model of long-term neuropathic pain. NeuroImage 2009;47:1007–14.

[50] Sprenger T, Willoch F, Miederer M, Schindler F, Valet M, Berthele A, Spilker ME, Forderreuther S, Straube A, Stangier I, Wester HJ, Tolle TR. Opioidergic changes in the pineal gland and hypothalamus in cluster headache: a ligand PET study. Neurology 2006;66:1108–10.

[51] Tsang A, Von Korff M, Lee S, Alonso J, Karam E, Angermeyer MC, Borges GL, Bromet EJ, Demytteneare K, de Girolamo G, de Graaf R, Gureje O, Lepine JP, Haro JM, Levinson D, Oakley Browne MA, Posada-Villa J, Seedat S, Watanabe M. Common chronic pain conditions in developed and developing countries: gender and age differences and comorbidity with depression-anxiety disorders. J Pain 2008;9:883–91.

[52] Wang J, Goffer Y, Xu D, Tukey DS, Shamir DB, Eberle SE, Zou AH, Blanck TJ, Ziff EB. A single subanesthetic dose of ketamine relieves depression-like behaviors induced by neuropathic pain in rats. Anesthesiology 2011; 115:812–21.

[53] Wester HJ, Willoch F, Tolle TR, Munz F, Herz M, Oye I, Schadrack J, Schwaiger M, Bartenstein P. 6-O-(2-[18F]fluoroethyl)-6-O-desmethyldiprenorphine ([18F]

DPN): synthesis, biologic evaluation, and comparison with [11C]DPN in humans. J Nucl Med 2000;41:1279–86.

[54] Williams FG, Mullet MA, Beitz AJ. Basal release of Met-enkephalin and neurotensin in the ventrolateral periaqueductal gray matter of the rat: a microdialysis study of antinociceptive circuits. Brain Res 1995;690: 207–16.

[55] Willoch F, Schindler F, Wester HJ, Empl M, Straube A, Schwaiger M, Conrad B, Tolle TR. Central poststroke pain and reduced opioid receptor binding within pain processing circuitries: a [11C]diprenorphine PET study. PAIN 2004;108:213–20.

[56] Zhang GF, Wang J, Han JF, Guo J, Xie ZM, Pan W, Yang JJ, Sun KJ. Acute single dose of ketamine relieves mechanical allodynia and consequent depression-like behaviors in a rat model. Neurosci Lett 2016;631:7–12.

[57] Zhang M, Kelley AE. Enhanced intake of high-fat food following striatal mu-opioid stimulation: microinjection mapping and fos expression. Neuroscience 2000;99:267–77.

[58] Zhang X, Bao L, Shi TJ, Ju G, Elde R, Hokfelt T. Down-regulation of mu-opioid receptors in rat and monkey dorsal root ganglion neurons and spinal cord after peripheral axotomy. Neuroscience 1998;82:223–40.

[59] Zhang X, de Araujo Lucas G, Elde R, Wiesenfeld-Hallin Z, Hokfelt T. Effect of morphine on cholecystokinin and mu-opioid receptor-like immunoreactivities in rat spinal dorsal horn neurons after peripheral axotomy and inflammation. Neuroscience 2000;95:197–207.

[60] Zubieta JK, Bueller JA, Jackson LR, Scott DJ, Xu Y, Koeppe RA, Nichols TE, Stohler CS. Placebo effects mediated by endogenous opioid activity on mu-opioid receptors. J Neurosci 2005;25:7754–62.

[61] Zubieta JK, Smith YR, Bueller JA, Xu Y, Kilbourn MR, Jewett DM, Meyer CR, Koeppe RA, Stohler CS. Regional mu opioid receptor regulation of sensory and affective dimensions of pain. Science 2001;293:311–15.

[62] Zubieta JK, Smith YR, Bueller JA, Xu Y, Kilbourn MR, Jewett DM, Meyer CR, Koeppe RA, Stohler CS. mu-opioid receptor-mediated antinociceptive responses differ in men and women. J Neurosci 2002; 22:5100–7.